NOAA Technical Report ERL 439–PMEL 39

Circulation and Property Distributions in the Central Bering Sea, Spring 1988

R.K. Reed
P.J. Stabeno

October 1989

U.S. DEPARTMENT OF COMMERCE
National Oceanic and Atmospheric Administration
Environmental Research Laboratories

NOAA Technical Report ERL 439–PMEL 39

Circulation and Property Distributions in the Central Bering Sea, Spring 1988

R.K. Reed
P.J. Stabeno

Pacific Marine Environmental Laboratory
Seattle, Washington

October 1989

U.S. Department of Commerce
Robert A. Mosbacher, Secretary

National Oceanic and Atmospheric Administration
John A. Knauss, Under Secretary for Oceans and Atmosphere / Administrator

Environmental Research Laboratories
Boulder, Colorado
Joseph O. Fletcher, Director

NOTICE

Mention of a commercial company or product does not constitute an endorsement by NOAA/Environmental Research Laboratories. Use of information from this publication concerning proprietary products or the tests of such products for publicity or advertising purposes is not authorized.

Contribution No. 1138 from NOAA/Pacific Marine Environmental Laboratory

For sale by the National Technical Information Service, 5285 Port Royal Road
Springfield, VA 22161

CONTENTS

Circulation and Property Distributions in the Central Bering Sea, Spring 1988

R.K. Reed and P.J. Stabeno

ABSTRACT. Data from a synoptic CTD survey in the central Bering Sea in winter 1988 are used to examine circulation and property distributions. A coherent, cyclonic circulation existed over much of the region. Geostrophic flow as great as 40 cm s^{-1} was present over the continental slope; another branch of relatively strong flow was situated over the shelf near a surface salinity front. The characteristic subsurface temperature minimum and maximum were both found in less dense water than in previous observations. Six satellite-tracked drifting buoys were also deployed. Their paths were in general agreement with the geostrophic flow, but some small eddies were revealed by the drifters that were not detected by the CTD data.

1. INTRODUCTION

Recently, data collected during summer and fall surveys in the central Bering Sea were used to examine circulation (Reed et al., 1988). These were preliminary surveys, preparatory to more detailed, interdisciplinary investigations. The present study analyzes results from a synoptic survey during spring, a season when data have generally been lacking. This work was conducted as part of the Fisheries Oceanography Coordinated Investigations of NOAA, whose goal is to gain understanding of the influence of various environments on recruitment of fish stocks.

Various data obtained from the NOAA ship *Oceanographer* during March–April 1988 are presented here. The upper-ocean circulation is inferred from the geostrophic relation, and physical property distributions are examined and discussed. Direct current measurements with satellite-tracked drifting buoys and an acoustic system are also analyzed. Finally, the major findings are discussed and compared with other results.

2. DATA AND METHODS

A total of 105 CTD (conductivity/temperature/depth) casts were taken in the region between Unalaska Island and the Pribilof Islands during 21 March–4 April 1988 (Fig. 1). A Neil Brown CTD system was used, and the data were recorded on disk in a minicomputer. Casts were taken to 1500 m or, in lesser depths, to within about 10 m of the bottom; data were recorded only during the downcast at lowering rates of 30–50 m min^{-1}. Temperature and salinity corrections were derived from data taken on almost all casts. Various routines were used to eliminate spurious data and to derive 1-m averages of temperature and salinity, which were used to compute density and geopotential anomaly.

Six satellite-tracked drifting buoys, with subsurface drogues (made of "holey-socks") centered at about 40 m, were deployed. Positions from the Argos satellite location system were used to derive buoy trajectories. The positions were edited, and a spline fit was used to obtain hourly data, which were low-pass filtered.

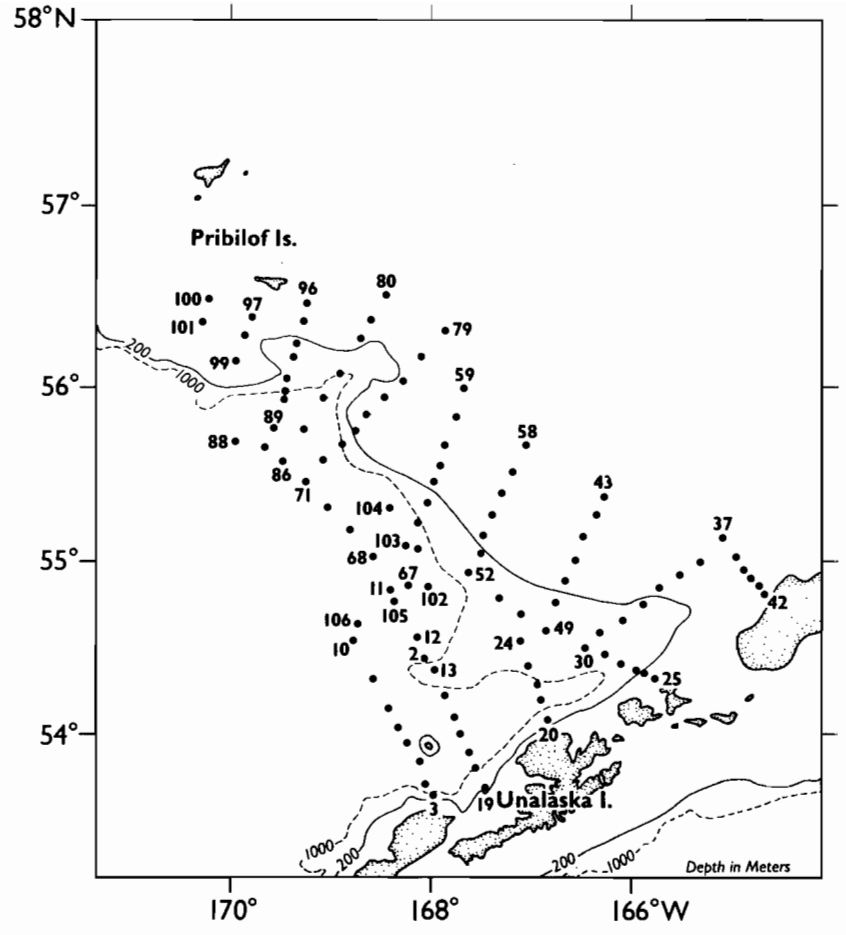

Figure 1. Locations of CTD casts taken in the central Bering Sea, 21 March–4 April 1988.

An RD Instruments acoustic Doppler current profiler (ADCP) was operated continuously on the ship's tracklines. Loran-C position data were recorded at 15-min intervals. The ADCP and position data were processed to derive along-track and across-track current components, which were averaged over 8-m vertical bins. Current profiles typically extended from about 20 to 300 m.

3. GEOSTROPHIC FLOW

Although CTD casts were taken to a maximum depth of 1500 m, considerably more data are available to depict circulation if a shallower reference level, such as 1000 m, is used. On the basis of previous studies, this choice is believed to be a reasonable one. Kinder et al. (1975) compared geostrophic calculations and direct measurements with drogues; they concluded that optimum reference levels varied between 800 and 1800 m and that speeds at 1000 m were less than 2 cm s^{-1}. Reed et al. (1988) found that use of 1000 m as a reference level gave surface flow patterns that were quite realistic. The baroclinic structure deeper than 1000 m is discussed further below.

The geopotential topography (ΔD) of the sea surface, referred to 1000 decibars (db; 1 db $\cong$ 0.98 m), is shown in Fig. 2a. A northeastward flow was present offshore of Unalaska

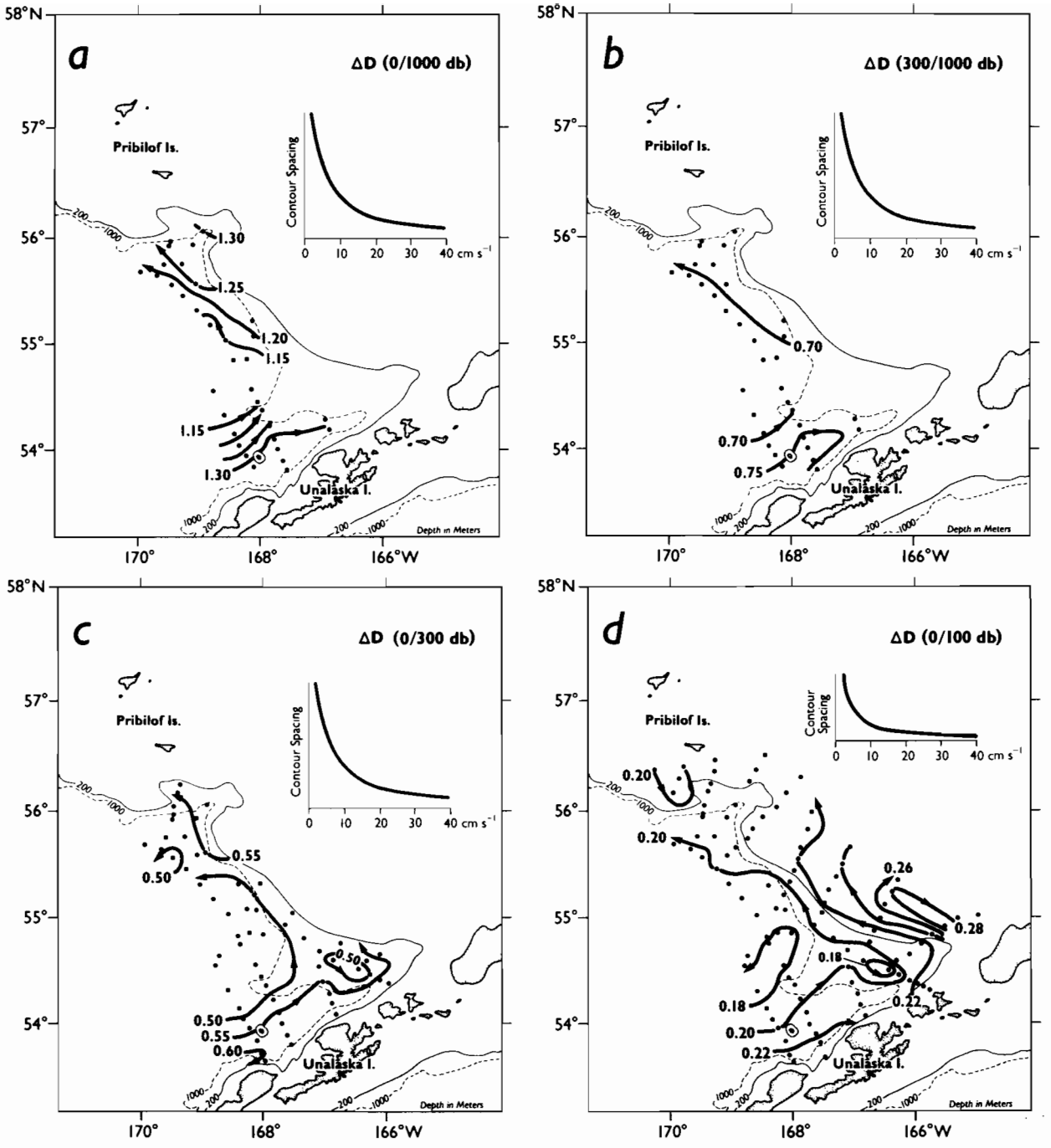

Figure 2. Geopotential topography (ΔD, dyn m) of (a) the sea surface (0 db), referred to 1000 db, 21–28 March 1988; (b) 300 db, referred to 1000 db, 21–28 March 1988; (c) the sea surface (0 db), referred to 300 db, 21 March–4 April 1988; and (d) the sea surface (0 db), referred to 100 db, 21 March–4 April 1988.

Island; it apparently turned to the northwest as it moved along the continental slope. Maximum speeds were about 30 cm s^{-1}. The simple pattern in Fig. 2a contrasts sharply with the patterns of Favorite and Ingraham (1973), Kinder et al. (1975), and Reed et al. (1988), which contained complex features with well-developed eddies. The topography at 300 db, referred to 1000 db, is

Table 1. Comparison of baroclinic structure above and below 1000 db

Stations*	ΔD_1 (0/1000 db), dyn m	ΔD_2 (1000/1500 db), dyn m	$\Delta D_2/\Delta D_1$, %
	March 1988		
5–9	+0.211	–0.017	–8
17–14	+0.076	–0.009	–12
65–67	+0.088	–0.003	–3
72–71	+0.067	–0.004	–6
84–86	+0.099	–0.019	–19
90–87	+0.065	+0.012	+18
	October – November 1986		
4–8	+0.156	+0.034	+22
45–50	+0.105	+0.020	+19
58–52	+0.168	+0.024	+14
61–64	+0.073	+0.018	+25
66–68	+0.074	+0.011	+15
72–70	+0.104	–0.003	–3

* Stations for the two periods are at different locations. The station order is arranged to give positive values of ΔD_1 (0/1000 db).

shown in Fig. 2b. The pattern of flow was quite similar to that at the sea surface, but the relief was only about half as great.

The geopotential topography of the sea surface referred to 300 db and 100 db is presented in Figs. 2c and 2d, respectively. In Fig. 2c, the flow appeared to intrude onto the slope, but it had a pattern similar to that in Fig. 2a. A small cyclonic eddy was present near 54.5°N, 166.5°W. Although the offshore relief in Fig. 2d was small, a well-developed northwestward flow, with speeds in excess of 20 cm s^{-1}, occurred over the shelf (inshore of the 200-m isobath). Schumacher and Kinder (1983) and Reed (1978) found that shallow reference levels gave realistic estimates of baroclinic flow over the Bering Sea shelf.

We earlier discussed the adequacy of 1000 db as a reference level for upper-ocean geostrophic flow computations. Deep, direct current measurements are lacking here, but baroclinic structure below 1000 db can be examined. Table 1 presents data on the relief across well-defined branches of flow as observed on this survey and also on one in this general area during fall 1986 (Reed et al., 1988). The area occupied by the 1988 survey was much smaller than the region sampled in 1986; thus the differences observed reflect both temporal and spatial changes.

During March 1988, the 1000/1500–db topography was generally a small percentage of the 0/1000–db relief; furthermore, the signs of ΔD above and below 1000 db differed, which indicates that baroclinic gradients above and below 1000 db had opposite directions. The data

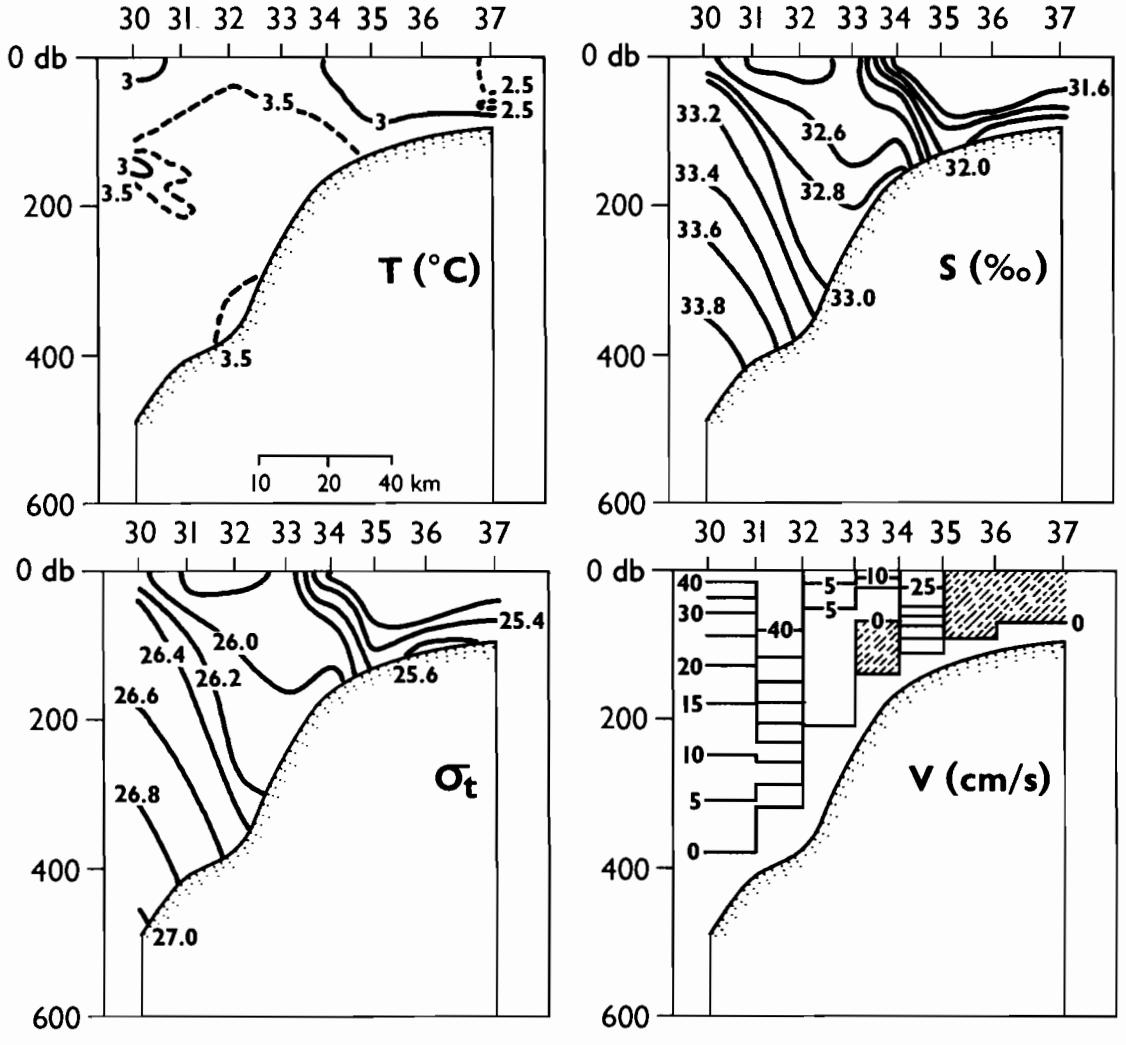

Figure 3. Vertical sections of temperature (°C), salinity (‰), sigma-t density, and geostrophic flow (cm s^{-1}, referred to the deepest common level between stations) for stations 30–37, 23–24 March 1988. Flow to the northwest is shown unhatched, and flow to the southeast is hatched.

from fall 1986 showed quite a different situation. The deep gradients were relatively larger than in March 1988, and gradients above and below 1000 db had the same sign. Thus the upper-ocean baroclinic structure in fall 1986 extended below 1000 db without reversals. These data sets do not allow an unequivocal determination of a level of no motion, but they indicate that the small relief below 1000 db is variable over space and time.

4. PROPERTY DISTRIBUTIONS

Vertical sections of temperature, salinity, sigma-t density, and geostrophic flow for stations 30–37 (see Fig. 1) are shown in Fig. 3. Sea surface temperature varied from about 2.5°C to almost 3.5°C. There was a general increase of temperature below the mixed layer, but secondary minima were also present (stations 30 and 31 especially). Surface salinity decreased from about 32.6 to less than 31.6‰ between stations 30 and 37. A sharp surface salinity front occurred

between stations 33 and 34. Since salinity largely controls density structure in the subarctic Pacific (Dodimead et al., 1963), the sigma-t section is very similar to the salinity section. Between stations 30 and 32, the strong sigma-t slopes indicate well-developed baroclinic structure, and the geostrophic flow section shows northwest flow in excess of 40 cm s^{-1}. Another zone of strong flow was present between stations 34 and 35, just shoreward of the surface salinity front.

Vertical sections of temperature, salinity, sigma-t density, and geostrophic flow for stations 71–79 (see Fig. 1) are presented in Fig. 4. As expected, surface temperature here was colder than that shown in Fig. 3, although values at the temperature maximum were similar at the two locations. Surface salinity was about 32.2‰, and no sharp surface front was present. A northwest flow with speeds greater than 20 cm s^{-1} was present between stations 71 and 73. Over the shelf, flow was weak and variable.

Horizontal distributions of various physical properties are presented in Fig. 5. The surface salinity distribution (Fig. 5a) indicates relatively saline water (>32.6‰) over a large offshore region north of 54°N and west of 168°W. This coincides with the low in geopotential topography (Fig. 2) around which the general cyclonic circulation occurred. In the eastern part of the region, a sharp surface salinity front was present; this is the "shelf-break" front separating the more saline slope waters and the fresher shelf waters (Schumacher and Kinder, 1983). The salinity distribution at 300 db (Fig. 5b) was quite similar to the patterns of geostrophic flow in Fig. 2.

The Bering Sea thermal structure is typified by a subsurface temperature-minimum layer, a temperature-maximum layer, and a gradual temperature decrease below 400 db. The temperature-maximum waters are not formed through local air-sea exchanges but result from horizontal advection of water from the North Pacific, especially through the deeper Aleutian Island passes (Sayles et al., 1979). The temperature-minimum layer, however, is formed by winter convection but persists year-round. Kinder et al. (1975) concluded that the major temperature minimum generally occurs on the sigma-t density surface of about 26.6 and that the temperature maximum lies at about sigma-t 26.8; Reed et al. (1988) found similar results in this general region. Although Sayles et al. (1979) showed some regional (and perhaps temporal) variability in the density of these temperature extrema, we did not anticipate that observations in spring 1988 would depart greatly from past conditions. Such was the case, however. The subsurface temperature minimum, which was generally colder than the sea surface, was at sigma-t 26.44 (±0.05), and the temperature maximum was at sigma-t 26.62 (±0.05). Thus the source waters that form the temperature maximum appeared to be atypical in spring 1988. The results also imply that convection during the winter resulted in temperature-minimum strata that were less dense and shoaler than normal. The early part of winter 1987–88 was relatively mild (Carol Pease, PMEL, personal communication, 1989), which supports this suggestion.

Figure 5c presents the temperature distribution at sigma-t 26.44, the mean density of the subsurface temperature minimum. A zone of water warmer than 3.5°C occurred just north of the Aleutian Islands; this relatively warm water in the southern part of the region might have been anticipated. To the north there was a broad zone of relatively cold water (<3.5°C), interrupted by small areas of warmer water. Farther north, however, the water was again generally warmer than 3.5°C. The overall pattern does not fit the concept of the temperature minimum being formed locally with its temperature varying inversely with latitude. An alteration of such a distribution by the geostrophic flow (Fig. 2) might account for the major features of the observed pattern, but several anomalies remain.

The temperature distribution at sigma-t 26.62 (the mean density of the temperature maximum) is shown in Fig. 5d. Although the range of temperature at this density was only about 0.2°C, there was enough variability that several intermittent zones of warm and cold water occurred in the southern part of the region. These are hard to reconcile with the pattern of flow, and this distribution seems generally more complex than found previously.

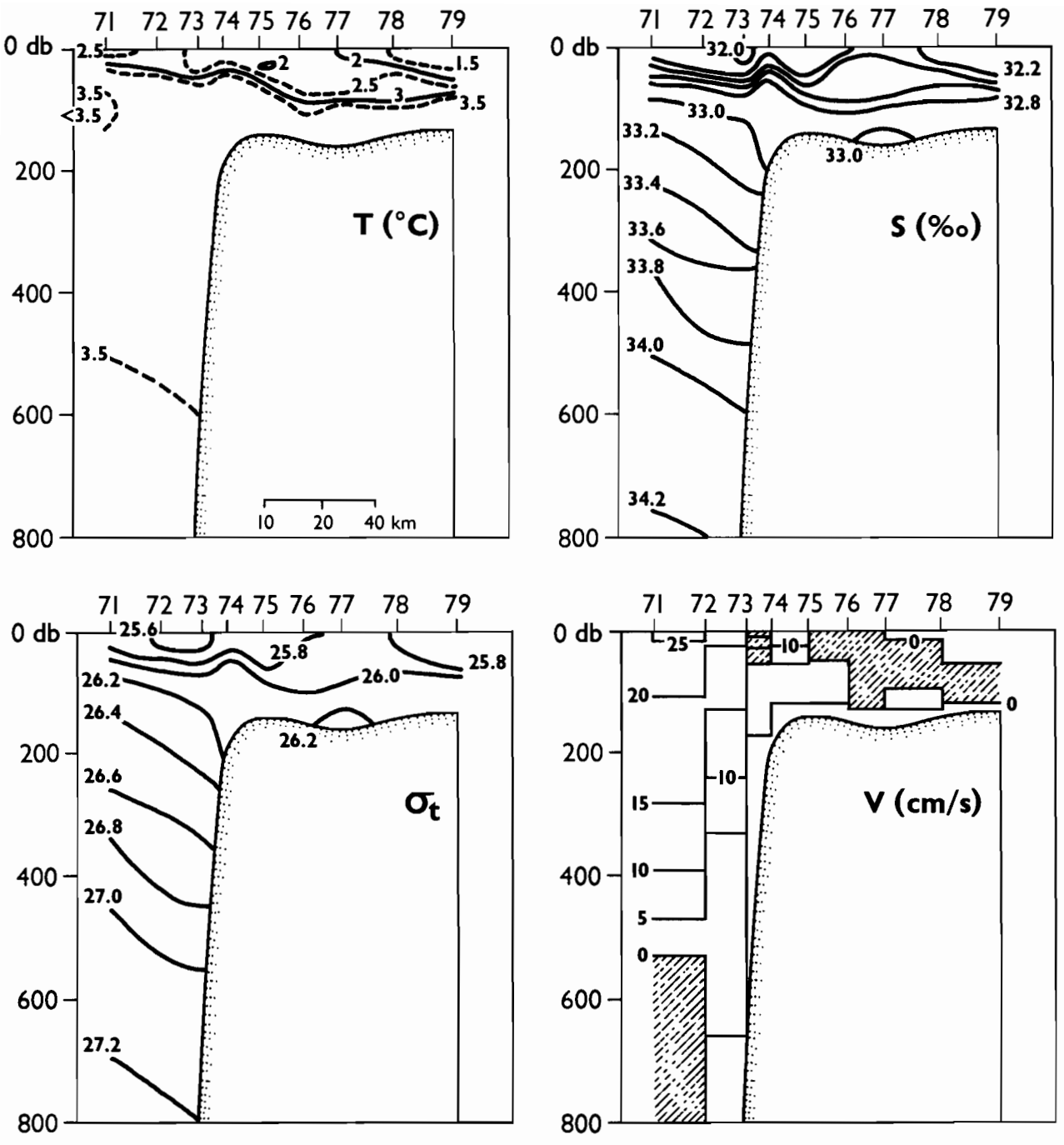

Figure 4. Vertical sections of temperature (°C), salinity (‰), sigma-t density, and geostrophic flow (cm s^{-1}, referred to the deepest common level between stations) for stations 71–79, 26–27 March 1988. Flow to the northwest is shown unhatched, and flow to the southeast is hatched.

5. DIRECT CURRENT MEASUREMENTS

Direct current measurements were made with (a) six satellite-tracked drifting buoys and (b) a shipboard acoustic Doppler current profiler. Some results are presented, discussed, and compared with the geostrophic flow.

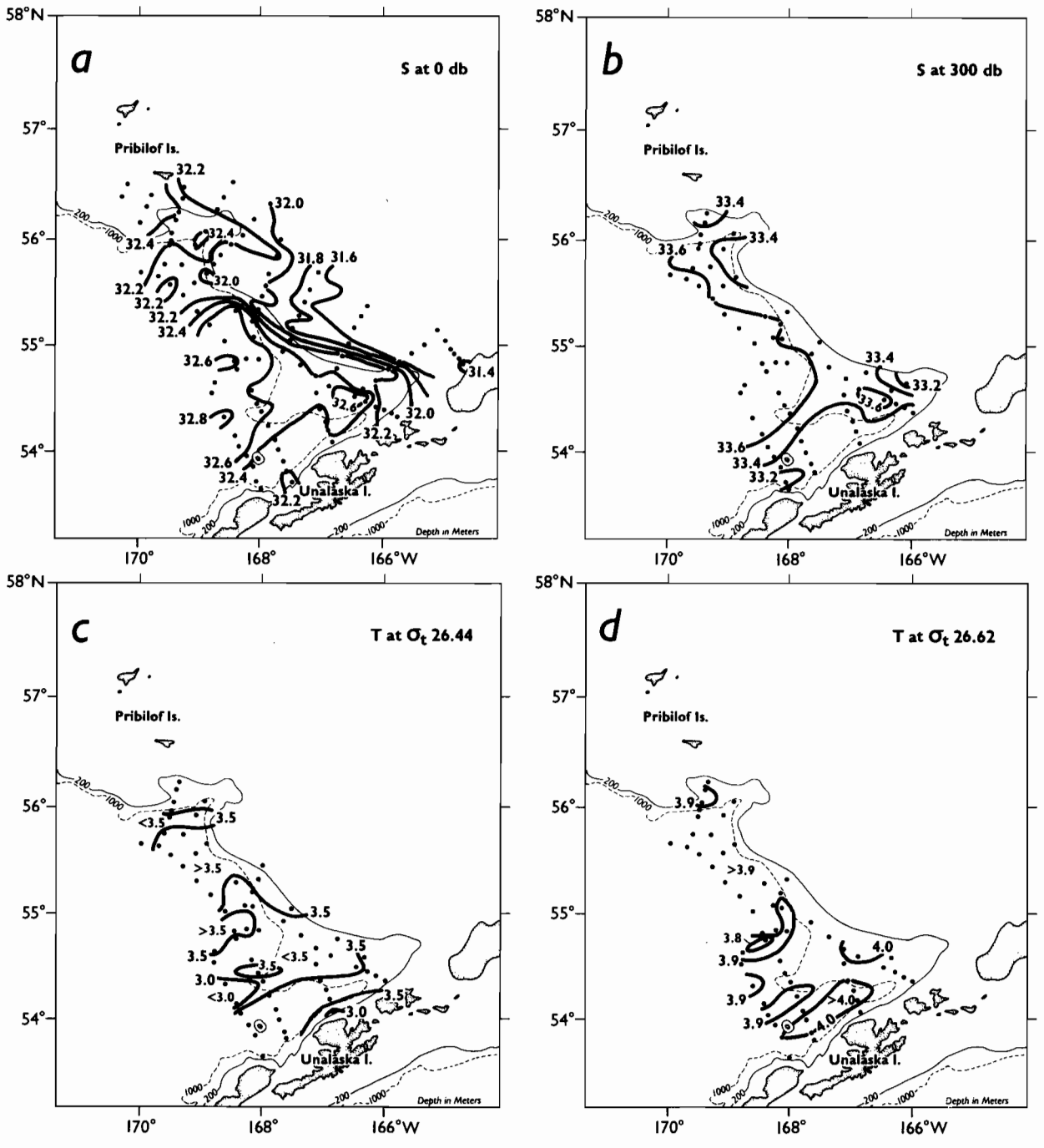

Figure 5. Horizontal distribution of (a) sea surface salinity (‰), (b) salinity (‰) at 300 db, (c) temperature (°C) at the sigma-t (σ_t) density surface of 26.44, and (d) temperature (°C) at the sigma-t (σ_t) density surface of 26.62, 21 March–4 April 1988.

5.1 Satellite-Tracked Drifting Buoys

The paths of the satellite-tracked drifting buoys, with drogues centered at about 40 m, are shown in Fig. 6, along with the 0/300–db geopotential topography. Buoys were deployed in three sets of two each. Buoys 7210 and 7211 were released near the northern extent of the CTD survey (Fig. 6a) on 27 March. The two drifters followed essentially the same path. They in-

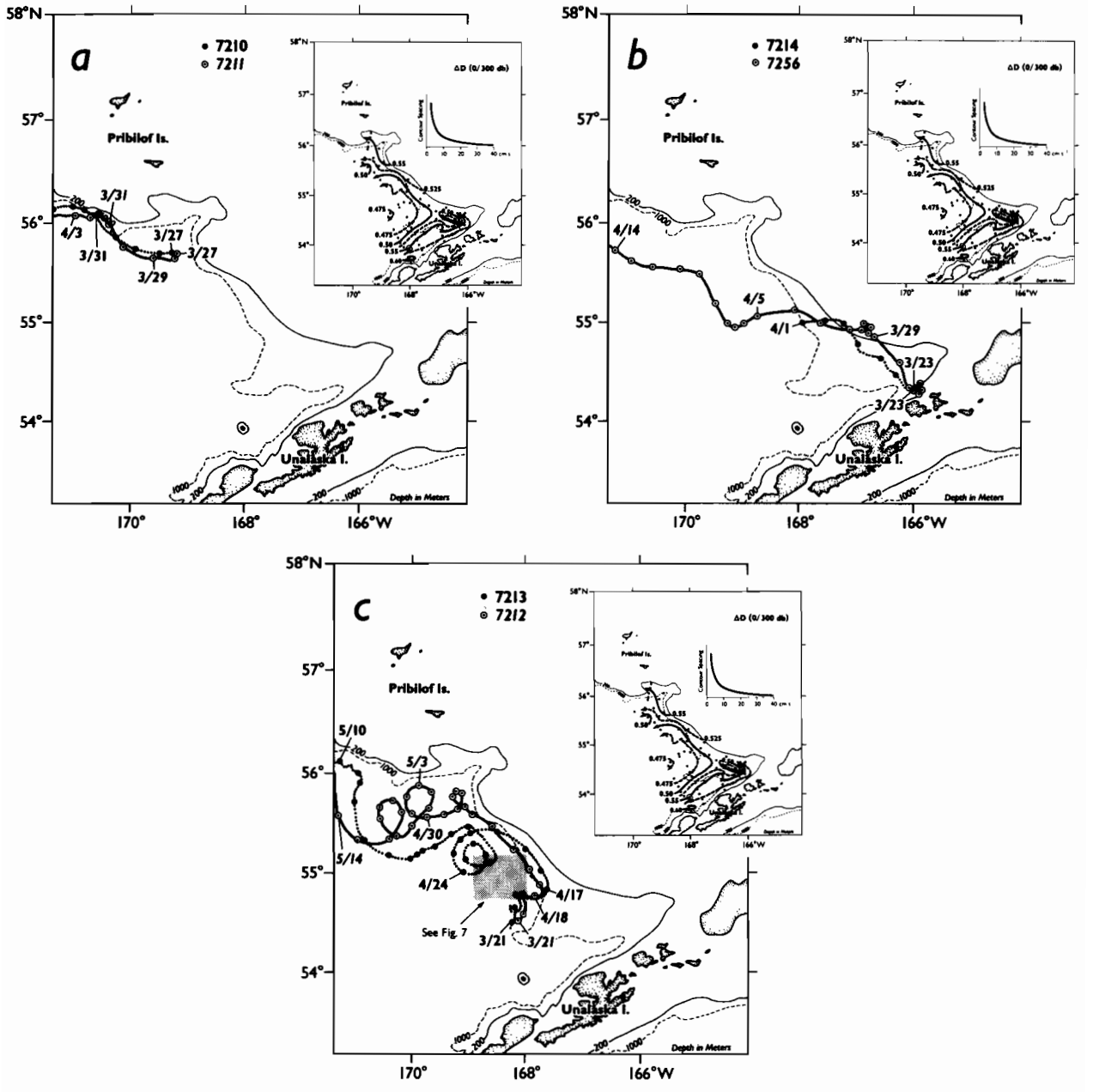

Figure 6. Trajectories of satellite-tracked drifting buoys: (a) buoys 7210 and 7211; (b) buoys 7214 and 7256; and (c) buoys 7212 and 7213. (Buoy tracks in the shaded area are shown in Fig. 7.) The positions each day (at 1200 UT; some dates shown) are plotted. The geopotential topography (ΔD, dyn m) of the sea surface (0 db), referred to 300 db, is shown in the inserts.

itially moved westward in relatively deep water but then followed the continental slope before exiting the area. The initial speed was about 25 cm s^{-1}; the surface geostrophic speed, referred to 300 db, was about 15 cm s^{-1}, but when referred to 1000 db, it was about 25 cm s^{-1} (Fig. 2a). Buoy 7256 traversed a large part of the area encompassed by the CTD survey, but its companion (buoy 7214) quit responding on 1 April (Fig. 6b). These buoys were deployed at the shelf break northeast of Unalaska Island on 23 March and moved very little for the first 3 days. They then traveled northward across the contours of geopotential topography, moved approximately along the geopotential isolines for about a week, and finally departed the survey area. The very strong

(~15 m s^{-1}) westward winds of 28–29 March (see Fig. 7) may account for the fact that the buoy paths crossed the contours of geopotential then. During 2–5 April, strong winds again occurred (see Fig. 7) and seem to have imparted a southward component of flow that led to buoy 7256 crossing the isolines of geopotential.

The most interesting behavior occurred with buoys 7212 and 7213 (Figs. 6c and 7). After deployment on 21 March, they soon entered an intense, small cyclonic eddy and remained in this feature for about 3 weeks. The eddy is not shown by the geopotential topography (Fig. 6c), but it was within a shear zone of opposing flows that perhaps was a factor in its formation. The daily evolution of the eddy, along with computed pressure-gradient winds, is presented in Fig. 7. The eddy appeared to have a very small radius (5–10 km) until about 27 March, after which it varied in size. The eddy translated somewhat erratically at speeds of about 2 cm s^{-1}, but particle speeds within the eddy were about 25 cm s^{-1}. It is not clear if the eddy actually moved appreciably or if the drifters began to leave the eddy as a result of the fairly strong winds in early April. Unfortunately, we have only the drifter tracks and winds derived from the pressure gradients. The lack of comprehensive, supporting data precludes any very definitive studies of the feature. After leaving the eddy and moving to the northwest along the continental slope, the buoy paths diverged (Fig. 6c). They both underwent some "looping" motion (anticyclonic and cyclonic) of short duration before finally exiting the area more than a month after the CTD survey.

5.2 Acoustic Doppler Current Profiler (ADCP)

In general, analysis of results from the ADCP suggests numerous problems with this data set. Vertical shear measurements from the ADCP in shallow water (~100 m) disagreed markedly with geostrophic estimates. This discrepancy may have been caused by the use of a wide-band filter setting; lack of agreement of flow over the shelf is also caused by tidal currents. The shears in deeper water were in closer agreement, but examination of shear structure suggests that the data from the ADCP had speed errors of at least 3 cm s^{-1}. This is a substantial error in a region of relatively weak currents, and therefore no ADCP results are shown.

6. DISCUSSION

The patterns of geostrophic flow in Fig. 2 indicate a very coherent, cyclonic circulation during this spring 1988 survey. This contrasts with previous studies that generally found numerous complexities and a flow rife with large eddies. The drifting buoy tracks shown here, however, revealed several small eddy-like features that were not resolved by the CTD survey. This finding is not an indictment of the geostrophic method, but it reflects the fact that the station spacing in our CTD survey was not able to detect the small (5–10 km radius) eddies present. The geopotential topography and direct current measurements were not entirely synoptic either, and strong winds at times seemed to impart a significant ageostrophic component to the drifter tracks.

Previous surveys in this area (Favorite and Ingraham, 1973; Kinder et al., 1975, and Reed et al., 1988) found numerous large eddies. The discovery of much smaller eddies in our data was an interesting finding. These features appear to be similar in scale to those prevalent in the Canadian Basin of the Arctic Ocean (D'Asaro, 1988; Aagaard, 1989). The eddies here also have large values of relative vorticity (~1.0×10^{-4} s^{-1} versus 1.2×10^{-4} s^{-1} for the planetary vorticity). Whereas the Arctic Ocean eddies are often not present at the sea surface and have thin vertical extent, they are quite long-lived (1 year or more), and they seem to be formed by stresses associated with flow over topographic features. It seems rather doubtful that the small eddies here have these characteristics.

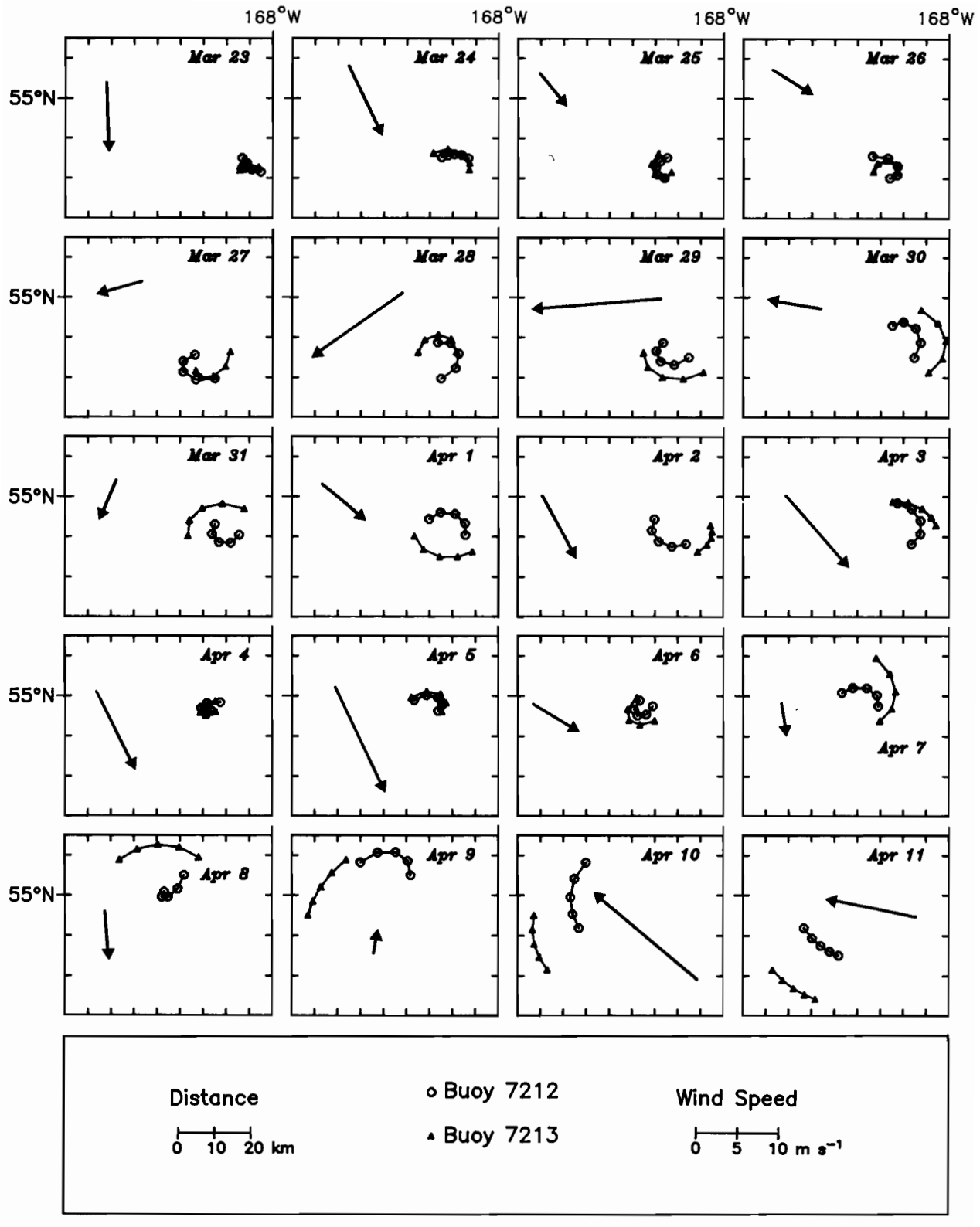

Figure 7. Trajectories of satellite-tracked drifting buoys 7212 and 7213, 23 March–11 April 1988. Positions were interpolated to six-hourly values. Wind vectors (at 1200 UT), derived from pressure gradients, are also shown.

We attempted to examine the vertical structure of baroclinic flow; the results imply that 1000 db may be a realistic reference level for near-surface geostrophic flow computations and that density slopes below 1000 db are small and variable. If this conclusion is borne out by subsequent data and analyses, it suggests a notable difference between this area and the subarctic region south of the Aleutian Islands. There, appreciable baroclinic structure extends downward to about 3000 db (Reed, 1984; Warren and Owens, 1988).

The data examined here indicate significant variations in the density of the characteristic temperature minimum and maximum surfaces. Considerable "winter climate" variability exists in this region of the Bering Sea. The Gulf of Alaska also exhibits a wide range of conditions (Xiong and Royer, 1984) that could affect the inflowing source waters that form the temperature maximum. Finally, we are surprised by the general lack of "finestructure" in temperature and salinity in our data over the outer shelf. Coachman and Charnell (1979) discussed finestructure in depths <200 m; here, however, such features were not present.

7. ACKNOWLEDGMENTS

We thank J. Gray for her enthusiasm and competence as Chief Scientist on this cruise. The efforts of the officers and crew of the NOAA ship *Oceanographer* are appreciated. J.D. Schumacher provided advice and support; C. DeWitt and P. Proctor assisted with the data preparation and analysis. This report is a contribution to the Fisheries Oceanography Coordinated Investigations of NOAA.

8. REFERENCES

Aagaard, K., 1989. A synthesis of the Arctic Ocean circulation. *Rapp. P.-V. Réun. Cons. Int. Explor. Mer 188*:11–22.

Coachman, L.K., and R.L. Charnell, 1979. On lateral water mass interaction – A case study, Bristol Bay, Alaska. *J. Phys. Oceanogr. 9*:278–297.

D'Asaro, E.A., 1988. Observations of small eddies in the Beaufort Sea. *J. Geophys. Res. 93*:6669–6684.

Dodimead, A.J., F. Favorite, and T. Hirano, 1963. Salmon of the North Pacific Ocean: Part II, Review of oceanography of the subarctic Pacific region. International North Pacific Fisheries Commission Bulletin No. 13, Vancouver, B.C., Canada, 195 pp.

Favorite, F., and W.J. Ingraham, Jr., 1973. Oceanography. Annual Report 1971, International North Pacific Fisheries Commission, Vancouver, B.C., Canada, 89–97.

Kinder, T.H., L.K. Coachman, and J.A. Galt, 1975. The Bering Slope current system. *J. Phys. Oceanogr. 5*:231–244.

Reed, R.K., 1978. The heat budget of a region in the eastern Bering Sea, summer 1976. *J. Geophys. Res. 83*:3636–3645.

Reed, R.K., 1984. Flow of the Alaskan Stream and its variations. *Deep-Sea Res. 31*:369–386.

Reed, R.K., J.D. Schumacher, and A.T. Roach, 1988. Geostrophic flow in the central Bering Sea, fall 1986 and summer 1987. NOAA Tech. Rep. ERL 433–PMEL 38, NOAA Environmental Research Laboratories, Boulder, CO, 13 pp.

Sayles, M.A., K. Aagaard, and L.K. Coachman, 1979. *Oceanographic Atlas of the Bering Sea Basin.* University of Washington Press, Seattle, 158 pp.

Schumacher, J.D., and T.H. Kinder, 1983. Low-frequency current regimes over the Bering Sea shelf. *J. Phys. Oceanogr. 13*:607–623.

Warren, B.A., and W.B. Owens, 1988. Deep currents in the central subarctic Pacific Ocean. *J. Phys. Oceanogr. 18*:529–551.

Xiong, Q., and T.C. Royer, 1984. Coastal temperatures and salinity in the northern Gulf of Alaska, 1970–1983. *J. Geophys. Res. 89*:8061–8068.

☆ U.S. GOVERNMENT PRINTING OFFICE: 1989—773-002/11,014 REGION NO. 8